A CRUSHABLE SHELL FOR SMALL BODY LANDERS

Silvio Schröder*(1), Christian Grimm(1), Lars Witte(1)
(1) DLR - German Aerospace Center - Institute of Space Systems, Robert-Hooke-Str. 7, D-28359 Bremen, Germany, Silvio.Schroeder@dlr.de

Abstract
This year the DLR built Mobil Asteroid Surface Scout (MASCOT) will decouple from the Hayabusa-2 spacecraft to perform surface science at the asteroid (162173) Ryugu. The MASCOT lander itself doesn't need a special damping system for touchdown since the asteroid is relatively small (Ø900 m) and therefore the surface gravity respectively the landing velocity is very low (few cm/s). In a next step DLR is developing further nano lander technologies for larger celestial bodies with respective higher surface gravity and therefore higher impact velocities. Previous investigations have shown that for larger bodies the landing velocity is in the range of 4 m/s which produces high shock loads.
A possible low complex and lightweight solution of damping the shocks is the use of a crushable shell around the lander. This crushable shell could be made out of aluminum honeycomb core with a High Performance Polyethylene cover sheet. The idea is to convert the kinetic energy into deformation work of the shell and reduce the shock load to the instrument platform. The design is particularly advantageous since no moving parts nor other mechanisms are required, thus making the system very robust and fail safe.
This paper is concentrating on a hardware test campaign recently done at DLR's Landing & Mobility Test Facility (LAMA). It will show the design of the shell, the test setup and the results of the campaign.

Keywords
Nano lander, space exploration, crushable structure, Landing & Mobility Test Facility (LAMA), DLR

1. INTRODUCTION

The MASCOT lander will touchdown on asteroid (162173) Ryugu with only a few cm/s and needs therefore no damping or protection system [1].

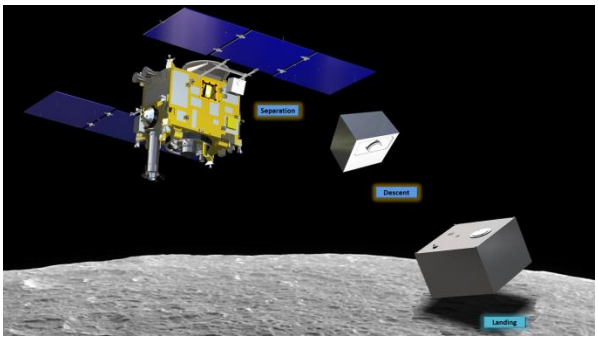

Figure 1: Artist view of MASCOT and Hayabusa-2

For higher landing velocities a system for absorbing the impact energy and protecting the lander and internal instruments is mandatory.
A possible low complex and lightweight solution of damping the shocks is the use of a crushable shell around the lander. This crushable shell could be made out of aluminum honeycomb core with a High Performance Polyethylene cover sheet. The idea is to convert the kinetic energy into deformation work of the shell and reduce the shock load to the instrument platform. The design is particularly advantageous since no moving parts nor other mechanisms are required, thus making the system very robust and fail safe.

2. DESIGN

As a baseline model for a nano lander the MASCOT lander was selected, which is 30x30x20 cm³ in size.
The lander has no guided attitude control during the descent and can land in any position, so all sides needed to be covered with crushable elements.
Since the honeycomb crash elements are only absorbing energy in one direction, each side had to be aligned accordingly. At the edges and corners the direction of the combs were 45° (see Figure 2).

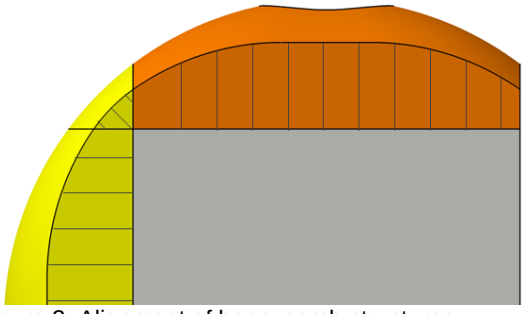
Figure 2: Alignment of honeycomb structures

The shape and density of the crash structure was defined by the touchdown conditions.
From this it follows that the impact does not necessarily go through the Center of Gravity (CoG) as can be seen in Figure 3.

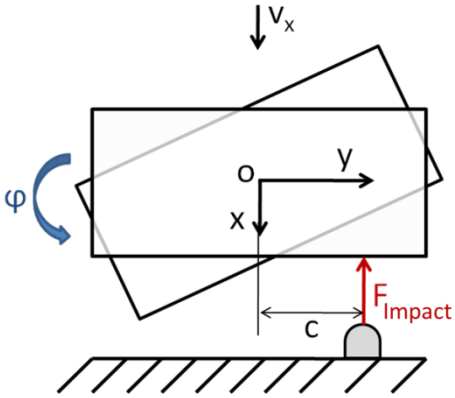

Figure 3: Scheme for calculating the mass distribution when impacting on an obstacle

The lander is rotating with the angle φ with respect to distance c between an obstacle and the landers CoG.
The initial conditions are given by

(1) $$F_{Impact} = m_{Lander} \cdot a = m_{Lander} \cdot \ddot{x}$$

and

(2) $$F_{Impact} \cdot c = J_{Lander} \cdot \ddot{\varphi}$$

Where F_{Impact} is the force acting on the lander, m_{Lander} the lander mass, $\ddot{x}$ the acceleration, J_{Lander} the moment of inertia and $\ddot{\varphi}$ the angular acceleration introduced to the lander.
After transposing and integrating of eq. (1) and (2) we are left with

(3) $$\dot{x}(t) = \frac{F_{Impact}}{m_{Lander}} t + v_x$$

and

(4) $$\dot{\varphi}(t) = \frac{F_{Impact} \cdot c}{J_{Lander}} t$$

It is further assumed that the angular rotation $\dot{\varphi}$ at the time of impact is equal to the negative velocity $\dot{x}$ divided by the distance c, since the lander will turn in the opposite way.

(5) $$\dot{\varphi}(t) = \frac{-\dot{x}(t)}{c}$$

By inserting eq. (3) and (4) into (5) we find

(6) $$\frac{F_{Impact} \cdot c}{J_{Lander}} t = \frac{-\left(\frac{F_{Impact}}{m_{Lander}} t + v_x\right)}{c}$$

Therefore the impact force is given by

(7) $$F_{Impact} = \frac{-v_x}{t} \cdot \frac{1}{\frac{c^2}{J_{Lander}} + \frac{1}{m_{Lander}}}$$

Since the first term is an acceleration the second term defines the mass distributions for the lander with respect of distance from its CoG.

(8) $$m(c) = \frac{1}{\frac{c^2}{J_{Lander}} + \frac{1}{m_{Lander}}}$$

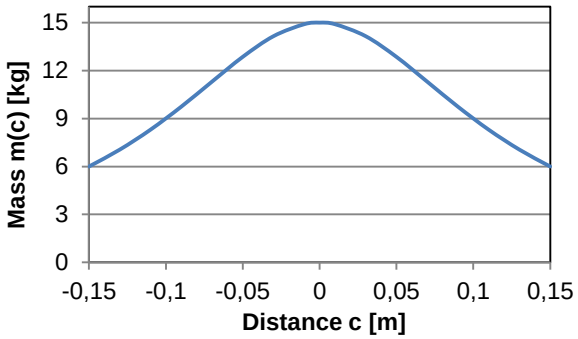

Figure 4: Calculated mass distribution of the impacting plate

For mass optimization of the crash structure it is therefore recommended to have a rounded shape with the maximum thickness in the middle and minimum on the edges.
Another important reason for using a rounded shape is the impact case on a flat plain. Since the impacted area for those cases are larger than on a stone the energy is absorbed in a much shorter crash stroke and leads to higher g-loads on the lander.
Another design factor which has to be taken into account are the cases where the lander hits a stone in an obliged angle. Even if the impact point is off-centered, the full mass is acting at the touch down point due to the velocity vector. So, despite of choosing a concave profile (like the mass distribution graph shows in Figure 3) we chose a convex profile to have more reserves in critical cases.

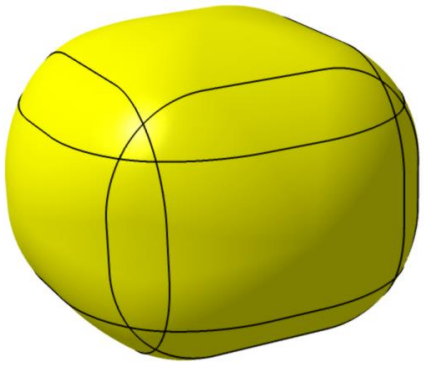
Figure 5: CAD model of the shell lander

The thickness of the crushable elements has been derived by the deceleration from 4 m/s to zero with an average g-load of 10g.

(9) $$h = \frac{v^2}{2a} = 0.08\ \mathrm{m}$$

Taking into account that the block length of the honeycomb is 20% of the original length, the chosen height of the honeycomb was set to 10 cm.

The crash material had to be selected to withstand either a landing on an even plain (maximum surface area) or on an obstacle (least surface area), where the first one is the critical case with a maximum of deceleration. The material has to be soft enough to not to produce high g-loads when the full surface is crushing, but stiff enough that a stone doesn't reach the block length of the honeycomb.

The dimensioning is driven by the kinetic energy E_{kin} needed to stop the mass m_{Lander} of the lander with its velocity v_x.

(10) $$E_{kin} = \frac{1}{2} m_{Lander} \cdot v_x^2$$

This energy has to be absorbed by crash material with:

(11) $$E_{kin} = W = V_i \cdot \sigma_{crash}$$

where V_i is the suppressed Volume of the honeycomb and σ_{crash} the crush strength of the material.
With the constraint of a maximum g-level of 40g, using eq. (9) we will get a minimum stroke of 2 cm (with 50% safety margin: 3 cm). The crashed Volume is then in the range of $5x10^{-4}$ m³ to $1x10^{-3}$ m³.

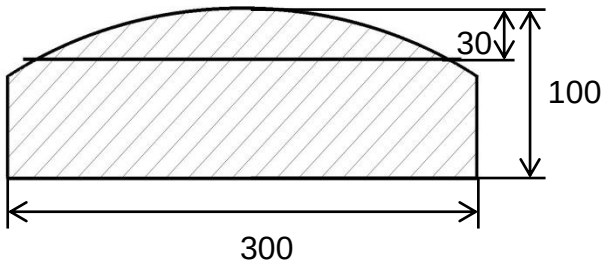

Figure 6: Cut view of a crash element

Inserting this in eq. (11) we find the crush strength to be

(12) $$\sigma_{crash} = \frac{E_{kin}}{V} = 0.12 \text{ to } 0.26\ \mathrm{MPa}$$

In the catalogue of a given manufacturer (e.g. Plascore [2]) the equivalent honeycomb is the PACL-XR1-1.0-3/8-.0007-P-5052 with a crush strength of 0.1725 MPa.

This procedure has been performed with all sides, edges and corners of the lander (see Table 1).

Table 1: Overview of the chosen honeycombs

Name	Application	Crush strength [MPa]
PACL-XR1-1.0-3/8-.0007-P-5052	Sides	0.1725
PACL-XR1-1.6-3/8-.001-P-5052	Short edges	0.3105
PACL-XR1-2.3-1/4-.001-P-5052	Long edges	0.6210
PACL-XR1-4.5-1/8-.001-P-5052	Corners	1.8975

For a better distribution of forces and for additional tensile strength, facesheets had to be applied to the crash elements. In earlier studies [3] the high-modulus polyethylene Dyneema® showed a good performance in impact tests, which is why this material has been chosen for the crash elements.
To prove the effectiveness of the facesheet the hardware tests have been performed with different numbers of layers ranging from zero to two.

3. TEST SETUP

Hardware testing has been performed using the Landing & Mobility Test Facility (LAMA) at the DLR Institute of Space Systems in Bremen [4]. LAMA has been configured to mount a pendulum with the attached demonstrator, which after release impacted either on a flat and hard surface or on a impacting body representing an obstacle on a rough surface. The velocity was set by the deflection and respective release height of the pendulum.

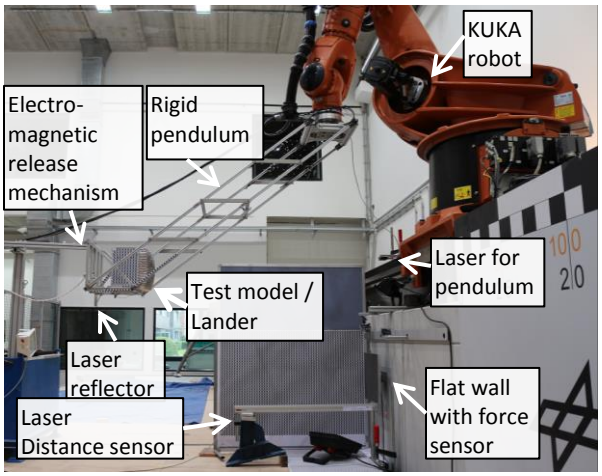

Figure 7: Shell lander test setup

The impact occurred when the pendulum reached maximum velocity at an angle of zero deflection. Test results have been recorded using force sensors, accelerometers, laser distance trackers and high speed camera data. This campaign focused on plane impact cases with dynamic crash and deformation behavior of the shell elements and determination of the absorbed energy while preventing any rotational movements of the lander before or after impact.
For this reason a rigid parallel pendulum has been used with stiffened cross-beams.

The test model with its pendulum has been trimmed to a reduced mass of 15 kg, while only one crush element was attached for each test.

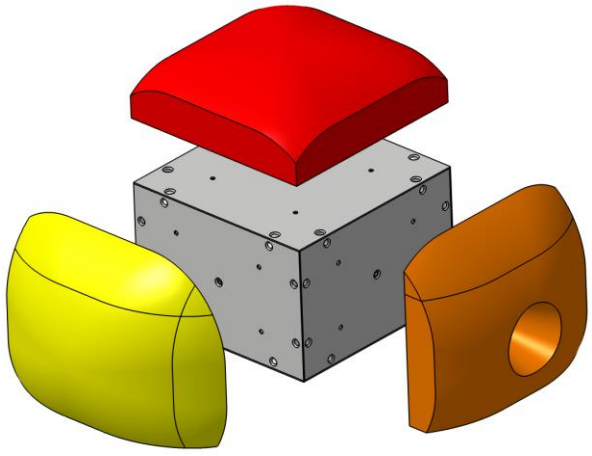
Figure 8: CAD-view of different crush elements

4. TEST EXECUTION

Test cases included impacts with the demonstrators' main planes (Top and Side) and Edges on either a penetrator (stone) or a flat surface.

Table 2: Shell lander test cases

	Penetrator	Flat
Top		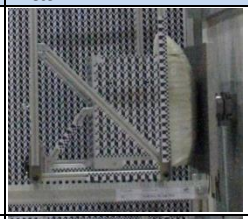
Side		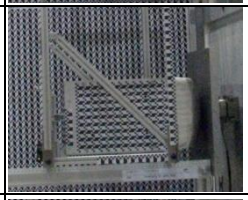
Edge	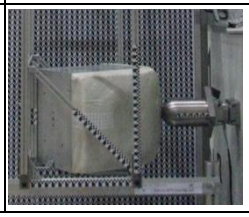	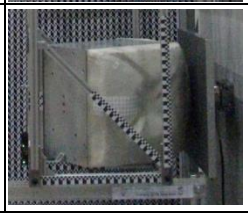

The tests have been performed using zero, one or two layers of facesheet material. The Velocities were set to 2, 3 and 4 m/s.

5. TEST RESULTS

In Figure 9 to Figure 12 one can see the general plots of the data output of a test run.

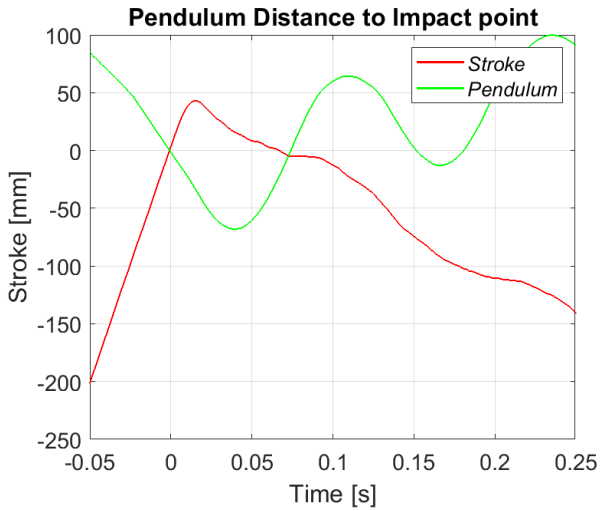

Figure 9: Laser distances for test case 2

In Figure 9 the distances of the test object and the pendulum are displayed. The offset was set to zero, when the pendulum is in vertical position

with the crash element touching either the flat wall or the penetrator.
One can see directly the maximum Stroke (red line) and the oscillation of the model afterwards. In contrast to that the pendulum has a larger deflection due to bending effects of the 2 m long bars. It also has a much stronger oscillation amplitude, but with the same frequency of about 8 Hz. This oscillating energy, which is transferred into the pendulum after impact and which is not absorbed by the crush elements is in the range of 15-35, depending on the impact type (flat or obstacle). This value has to be taken into account when analyzing the final amount of energy which has been absorbed by pure mechanical deformation within the crush elements.

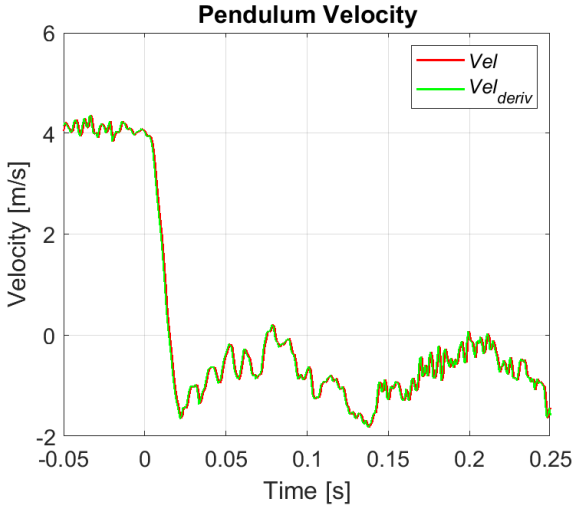

Figure 10: Derived velocity for test case 2

The velocity has been derived from the Laser distance sensor. One can see that the target velocity of 4 m/s was met quite accurately and that the oscillation started right after the crash element lost contact to the penetrator (27 ms after impact, see also force data in Figure 11). However the impact velocity of the lander was a little bit lower, because of the vertical distance between laser reflector and impact point.

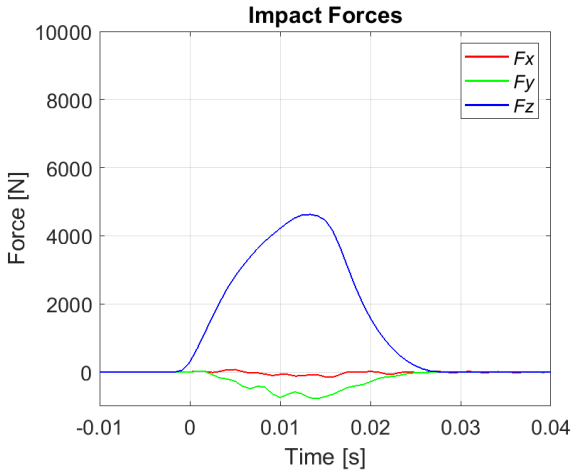

Figure 11: Impact forces for test case 2

The impact force shows an increasing progress until the maximum stroke (15 ms) and then a faster decreasing afterwards.

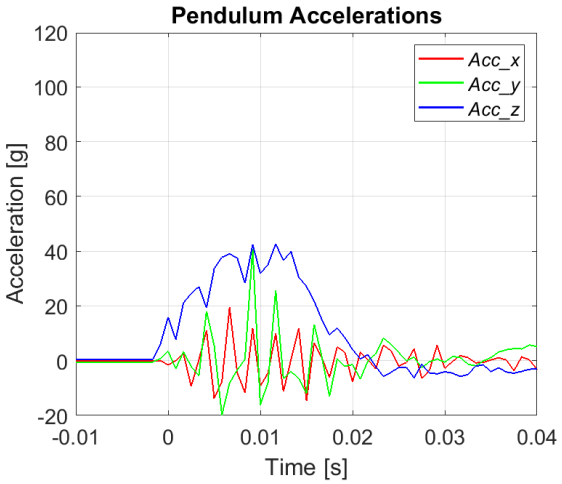

Figure 12: Impact accelerations for test case 2

The same behavior applies to the acceleration data. One can see that the maximum deceleration is close to 40g which was the design goal. But not every test case fulfilled the g-load requirement (especially the flat impacts) as can be seen in Figure 15.

The impacted objects (Figure 13) crashed as expected. Impacts on a flat surface produced a quadratic impact zone (b) and impacts on a penetrator a spherical one.

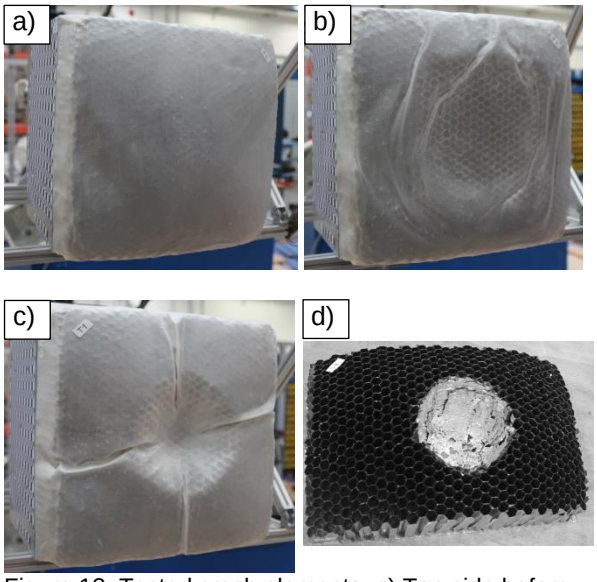

Figure 13: Tested crash elements: a) Top side before crash, b) Top side after flat impact, c) Top side after penetrator impact, d) side element after penetrator impact without facesheet

The influence of the facesheet is clearly seen in comparison of (c) and (d) where the objects hit the penetrator at the same speed. While case (c) has a moderate impact stroke of 53 mm, case (d) went completely through until the penetrator reached the backplane of the element.
Impacts with two facesheets on the opposite side had lower impact strokes and therefore produced higher accelerations. A comparison of the influences of number of laminates can be seen in Figure 14.

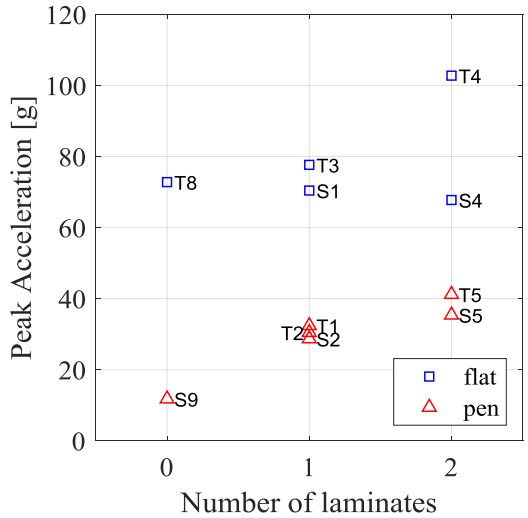

Figure 14: Comparison of number of facesheet laminates

As for impact cases on a flat surface only a minor influence of the facesheets is seen, but for impacts on an obstacle this effect is much more dominant. The more laminates you have the higher is the added crush strength and therefore the acceleration.

As a result it can be stated that a facesheet is necessary to prevent an obstacle of hitting through the honeycomb, but not a too stiff one to not have too high crush strength.

For impacts on a flat surface the velocity is more important than the number of laminates as can be seen in the blue markers of Figure 15 (Indices name the number of laminates).

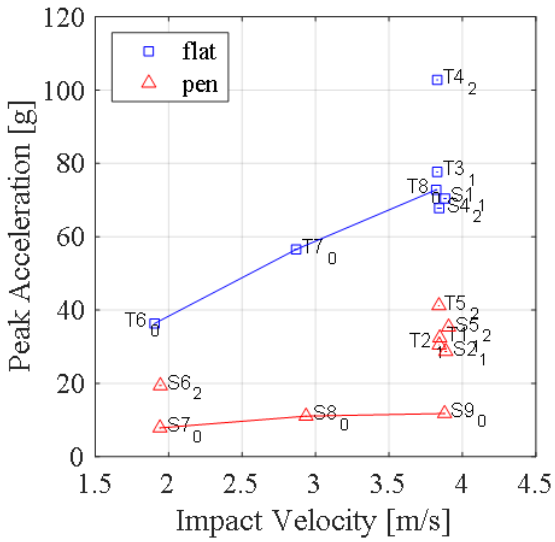

Figure 15: Comparison of tests with different velocities

The red and blue lines mark the trend of crush-elements with same numbers of laminates (Index 0).
It therefore has to be stated that the impact velocity is crucial for the peak-loads on the system. This is the critical parameter for the definition of the crush strength.

In Figure 16 the impact energy over the crush energy is plotted. The impact energy is derived by eq. (10) and is only dependent from the impact velocity. The crush energy is the energy balance before and after the impact taking into account the induced oscillation within the pendulum.

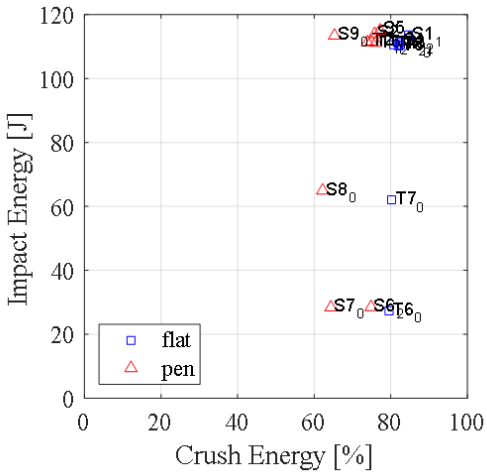

Figure 16: Impact energy vs. absorbed energy for different test cases

As can be seen, the crush energy is independent by the impact velocity and is only driven by the structural build-up of the crash elements. In these tests we were able to reduce the impact energy by about 80%.

6. CONCLUSION & OUTLOOK

The department of Landing & Exploration Technology of the DLR Institute of Space Systems successfully developed a crushable shell for a nano lander. The design and choice of material was driven by a specific scenario of landing a 15 kg object with 4 m/s on an airless body.
In an experimental setup where the lander crashed horizontally against a vertical obstacle the construction has been proved, so that this shell lander concept achieved a Technology Readiness Level (TRL) of 4.
The results showed a strong proportional dependence of the velocity for impacts for both on a flat surface as well as on an obstacle; the higher the impact speed, the higher the peak accelerations. For the design of a future mission, precise information about the landing velocity is necessary.
Another important result of this campaign is fact that the absorbed energy of the impact is independent from the velocity.
Other influences for the design are the conflictive requirements of landing on a flat surface to landing on a stone. A flat surface requires a preferably low crush strength, while a touchdown on a stone requires a harder material because of the small crushing area. The best compromise for both constraints is therefore a soft core material with a high tensile strength facesheet.

Because of the limited amount of test models only certain aspects could be investigated. This leaves open gaps to other questions. How will the lander behave for inclined impact cases and how is the landing dynamic in a realistic gravity environment when the lander can freely rotate over all axes?
In the test campaign we only used Aluminum Honeycomb material, but there are probably other crash materials which might be better, especially multi-directional ones.
Finally this campaign also didn't answer the question of how the shell could be released from the lander, since the scientific instruments need an open view to the surface.
These and other questions will be addressed in ongoing numerical simulations as well as in additional laboratory tests [5].

7. REFERENCES

[1] Ho, T.-M., Baturkin, V., Grimm, C.D., et al. „MASCOT—The Mobile Asteroid Surface Scout Onboard the Hayabusa2 Mission", Space Science Reviews 208.1, pp. 339–374, 2017

[2] Plascore CrushLite, https://www.plascore.com/de/download/datasheets/energy_absorption_documentation/Plascore_CrushLite.pdf, 08/2018

[3] Reinhardt, B., Experimental Investigation and Evaluation of the Crash Behaviour of a Planetary Landing Platform Using Crushable Layers of Aluminum Honeycomb, Bachelor Thesis at University of Bremen, 2012

[4] Schröder, S., Applications for a gravity compensating test facility for planetary surface mobility, DLRK, 2011

[5] Grimm, C.D, Schroeder, S., Witte, L. et al., Size Matters - The Shell Lander Concept for Exploring Medium-Size Airless Bodies, Proceedings of the International Astronautical Congress (IAC), Bremen, 2018